Chemical Engineering Journal 400 (2020) 125853

Contents lists available at ScienceDirect

Chemical Engineering Journal

journal homepage: www.elsevier.com/locate/cej

Visible-light-excited humic acid for peroxymonosulfate activation to degrade bisphenol A

Jialin Jia[a], Dongmei Liu[a,*], Jiayu Tian[b,*], Wei Wang[a], Jiaxin Ni[a], Xin Wang[a]

[a] School of Environment, Harbin Institute of Technology, Harbin 150090, China
[b] School of Civil Engineering and Transportation, Hebei University of Technology, Tianjin 300401, China

HIGHLIGHTS

- Visible light (VL) excited HA can activate the PMS to generate reactive species.
- $^1O_2$ was the main reactive species for BPA degradation in PMS/HA/VL system.
- HA was damaged and transformed to the low weight molecular fractions.
- Phenolic groups of HA played the role of electron-donator.
- Quinone moieties of HA accelerated the electron-transfer between HA and PMS.

GRAPHICAL ABSTRACT

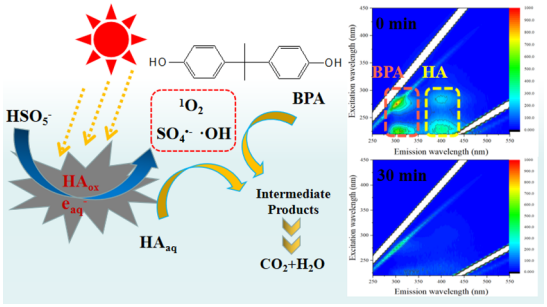

ARTICLE INFO

Keywords:
Peroxymonosulfate
Visible light
Humic acid
Bisphenol A
Singlet oxygen

ABSTRACT

In this study, a novel peroxymonosulfate (PMS) activation method by visible light (VL) excited humic acid (HA) was developed and applied to degradation of bisphenol A (BPA). Results showed that, in HA (2 mg/L)/PMS (1 mM)/VL system, the degradation rate of BPA could reach 95.4% within 30 min, which was much higher than that of HA/VL system (9.4%) and PMS/VL system (15.5%). Meanwhile, the concentration of HA was also decreased in this process and the original structure of HA was obviously destroyed. Reaction mechanism accounting for the effect of HA on BPA degradation in the PMS/HA/VL system was explicated by the quenching experiments, electron paramagnetic resonance (EPR) detection and HA fractionation experiments. Results showed that singlet oxygen ($^1O_2$), hydroxyl radical (·OH) and sulfate radical ($SO_4^{\cdot-}$) were all involved in the system, and $^1O_2$ was the primary reactive species responsible for BPA degradation. The aromatic constituents of HA made the dominant contribution to the generation of reactive species, in which the phenolic groups played the role of electron-donor, and the quinone moieties acted as the electron shuttles could accelerate the electron-transfer between HA and PMS, which thus activated PMS to form the reactive species for BPA degradation. As HA is ubiquitous in nature, this study may provide a new insight into the in situ water treatment with the assistance of PMS.

1. Introduction

Recent years, peroxymonosulfate (PMS)-based advanced oxidation process has been widely used for removal of emerging contaminants due to its superior oxidation capacity and chemically stable for convenient transportation and storage [1]. A variety of methods have been proposed to activate PMS such as heat [2], ultrasound [3], ultraviolet [4], carbon materials [5], metal oxides [6], transition metals

* Corresponding authors.
E-mail addresses: ldm819@126.com (D. Liu), tjy800112@163.com (J. Tian).

https://doi.org/10.1016/j.cej.2020.125853
Received 8 March 2020; Received in revised form 6 June 2020; Accepted 8 June 2020
Available online 12 June 2020
1385-8947/

[7], base [8], quinone and phenols [9]. However, these methods either require the excess energy/chemical input, or may provoke inevitable secondary pollution to the environment, which may be not appropriate to the practical application. Photochemical activation of PMS represented by ultraviolet (UV) has been investigated [10,11], but a more moderate photochemical activation with VL is much desirable since VL accounts for a larger proportion of the solar spectrum than UV light. Some photocatalysts such as TiO_2 [12], $BiVO_4$ [13] and $ZnFe_2O_4$ [14] have been reported to effectively activate PMS under VL irradiation, but these photocatalysts are not very suitable for practical water treatment due to the complex preparation methods and tedious separation process. Thus, a simple, effective and environmentally benign method for PMS activation by utilizing VL is still urgently needed at present.

Humic acid (HA) is a kind of yellow-to-black colored macromolecular natural organic matter (NOM) which owns a high content (50–60%) of aromatic carbon or hydrocarbon, containing rich oxygen-containing functional groups such as carbonyl, carboxyl, nitroso, amino, hydroxyl and phenolic groups [15,16]. HA is ubiquitously exists in water bodies and soils which was usually regarded as the organic pollutants [17], however, it also plays the important role in some advanced oxidation processes (AOPs). Under the UV–vis light irradiation, HA can be excited to generate reactive intermediates such as superoxide ($O_2^{\cdot -}$), singlet oxygen ($^1O_2$), the triplet excited state of HA* (^{3}HA*), and hydrated electrons (e_{aq}^-) [18,19]. These reactive intermediates have been reported to be able to enhance the degradation of the organic pollutants in AOPs. For example, Cho et al. [20] found that as a photosensitizer or an electron donor, HA could eject e_{aq}^- from its excited state to the conduction band of TiO_2 under VL irradiation, which resulted in the degradation of CCl_4 through a series of electron transfer reactions. Yao et al. [21] reported that under VL irradiation, fluvic acid (one kind of humic acid) can be excited, and then activate the dissolved oxygen to form $O_2^{\cdot -}$, which further reacted with Mn(II) to produce Mn (III) for the enhanced degradation of BPA. The similar activation function was also found by Wang et al. [22] in VL irradiated HA/Mn(II) system. Besides, Guo et al. [23] and Dunnivant et al. [24] found that the quinone moieties of HA can be photo-induced and then served as the electron shuttles to transfer electrons for participating in a series of redox reactions. Considering that HA can produce e_{aq}^- under VL irradiation, and the quinone moieties of HA can be served as the electron shuttles to transfer the electrons, the VL excited HA might activate the PMS to form reactive oxygen species (ROS) for the degradation of organic pollutants. However, up to now, there has been no study about it. If PMS can be activated by the VL excited HA, it would be a more economic PMS activation method, because it can avoid the use of various catalysts and the subsequent separation process.

Therefore, in this study, the VL excited HA was employed to activate PMS for degrading organic pollutants for the first time. BPA, one of the most common endocrine disruptor which frequently detected in the environment was chosen as the substrate pollutant to evaluate the catalytic performance of the PMS/HA/VL system. The reactive species in the system were identified by the quenching tests and EPR characterization. Besides, HA was fractionalized to different molecule size fractions for further exploring the reaction mechanism, and a possible mechanism as well as the BPA degradation pathways were subsequently proposed. Finally, the effect of operating parameters and water matrices on BPA degradation were also evaluated. The results of this study suggested that a novel PMS activation approach by VL excited HA was developed for water treatment.

2. Experimental

2.1. Materials and reagents

Humic acid (HA, > 99% purity), bisphenol A (BPA, 99%), PMS (available as Oxone $KHSO_5{\cdot}0.5KHSO_4{\cdot}0.5K_2SO_4$), and 5,5-dimethyl-1-pyrroline N-oxide (DMPO, 97%) were purchased from Aladdin Chemistry Co., Ltd (China). Furfuryl alcohol (FFA, 98%) and 2,2-azinobis(3-ethylbenzothiazoline)-6-sulfonic acid diammonium (ABTS, 99%) were obtained from Sigma-Aldrich Co., Ltd (USA). 9,10-diphenylanthracene (DPA, 99%) and 2,2,6,6-Tetramethyl-4-piperidinol (TMP, 99%) were obtained from J&K Scientific Ltd (China). Methanol (MeOH), *tert*-butanol (TBA), and acetonitrile of HPLC grade were obtained from Tedia and Fisher Co., Ltd (USA). Other reagents of analytical grade were purchased from Sinopharm Chemical Reagent Co., Ltd (China). HA and DPA stock solutions were prepared according to the previous literatures [25,26]. The ultrafiltration (UF) membranes employed for fractionation were made of regenerated cellulose and obtained from Millipore (USA). Three types of membrane with molecular weight cutoffs (MWCOs) of 5, 30, 100 kDa were used in this work.

2.2. Fractionation of HA

An UF fractionation method was used to separate HA into four molecular size fractions of < 5 kD, 5–30 kD, 30–100 kD, and > 100 kD to study the effect of molecular size and chemical composition of HA on BPA degradation. The stock HA solutions (500 $mg{\cdot}L^{-1}$, 500 mL) were firstly prepared in deionized water and filtered through 0.45 μm cellulose acetate membranes. Then the UF membranes with different MWCOs were used to separate the filtered water sample, this process was conducted under a constant pressure of 0.1 MPa. To prevent cake layer formation and reduce concentration polarization, UF experiments were conducted with a stirrer running at 250 rpm. Fractionation was conducted in triplicate to keep the errors below 3%.

2.3. Catalysis experiments

Photocatalytic experiments were carried out in a 100 mL beaker which contained 50 mL aqueous solution of BPA (10 mg/L) under magnetic stirring. A 300 W xenon lamp (Beijing NBeT) with a 400 nm cut-off filter was employed as the visible light source. The light intensity irradiated on the surface of solution measured with an optical power meter (Model: FZ-A) was 70 $mW{\cdot}cm^{-2}$, with the sensor was placed at the same height (10 cm) as the solution surface from the light source. The reaction was triggered by introducing certain amount of PMS and HA into the beaker with the xenon lamp switched on. The pH of the solution was adjusted by 1.0 M H_2SO_4 or NaOH solution. The temperature of the reaction system was kept at 25 ± 0.5 °C with continuous circulation cooling water (Fig. S1). At desired time interval, the reaction solution was withdrawn and filtered through 0.22 μm membranes, then 1 mL of the filtrated sample was injected into a brown vial which contained 0.5 mL of 1 M sodium thiosulfate solution to terminate the reaction. For HA concentration measurement, 2 mL reaction solution was withdrawn and filtered with a 0.45 μm membrane filter, then the filtrate was poured into a centrifuge tube contained 1 mL of 1 M sodium thiosulfate solution to stop the reaction. The degradation rate of both BPA and HA was estimated by a kinetics equation:

$$\ln(C_t/C_0) = kt$$

where C_t and C_0 are defined as the BPA/HA concentration at the certain time and the initial BPA/HA concentration, respectively, t is the reaction time, and k is the reaction rate constant [27]. All experiments were performed in duplicates or triplicates, and the average values with their standard deviations were recorded.

2.4. Analytical methods

The BPA concentration was measured by the UPLC system (Waters, MA, USA) with a BEH C18 column (1.0 × 50 mm, 1.7 μm) and an UV detector (λ = 230 nm). The mobile phase consisted of 65% MeOH and 35% ultrapure water with a flow rate of 0.1 mL/min. The degradation

intermediates of BPA were identified by an ultra-performance liquid chromatography/MS/MS (Acquity UPLC, XEVO TQ MS) coupled with a triple quadrupole detector (Xevo TQ-S) at ESI negative ionization mode. The identification of reactive species was conducted on an Electron paramagnetic resonance (EPR, Bruker A200 spectrometer, Germany). Determination of $DPAO_2$ was carried out on a HPLC/APCI-QqQMS based on the previous study [28]. HA concentration was evaluated by recording the UV absorption at 254 nm (UV_{254}) using an UV–vis spectroscopy (2550, Shimadzu, Japan). Besides, $SUVA_{254}$, which is the absorption of light at 254 nm per unit of carbon was also characterized, and DOC was measured by a TOC Analyzer (Kyoto, Shimadzu, Japan). The PMS decomposition was followed by a colorimetric method (Text S1). The key organic functional groups of HA was characterized by Fourier transform infrared spectroscopy (FT-IR) (Prestige-21, Shimadzu, Kyoto, Japan). The structural changes of HA during the reaction process were determined by a three-dimensional (3D) fluorescence spectrometer (F7000, Hitachi, Japan), both the excitation (Ex) and emission (Em) slits were adjusted to 5 nm. The emission and excitation spectra were scanned from 200 nm to 450 nm at 5 nm intervals and 250 nm to 550 nm at 1 nm intervals, respectively, with the scanning speed of 30000 nm·min^{-1}. The size fraction of HA was determined by using a high-pressure size exclusion chromatography with a UV detector (HPSEC/UV) and a TSK-gel G4000PWXL silica gel column (7.8 × 300 mm, 10 mm) (TOSOH, Japan). The mobile phase consisted of 0.002 mol/L K_2HPO_4, 0.002 mol/L KH_2PO_4, and 0.1 mol/L NaCl (phosphate buffer solution, pH = 6.85).

3. Results and discussion

3.1. Degradation efficiency of BPA in PMS/HA/VL system

The degradation efficiencies of BPA in different systems were studied and compared to explore the role of HA on BPA degradation in PMS/HA/VL system. As can be seen in Fig. 1a, the BPA degradation in the absence of PMS and HA (control group) was negligible, which precluded the possibility of self-degradation due to dissolved oxygen in the solution or photolysis [29]. The introduction of PMS led to about 15.5% removal of BPA within 30 min under VL irradiation, and this value exhibited only a slight difference from that of the PMS/dark system, which thus ruled out the possibility of PMS activation by VL individually. Besides, the degradation efficiency of BPA in the PMS/HA/dark system was only 11.3% within 30 min, suggesting that HA exhibited fairly weak ability to activate PMS without light irradiation. For the HA/dark and HA/VL groups, the BPA degradation rate was shown to be only 8.6% and 9.4%, respectively. This indicated that there was almost no interaction between HA and BPA with or without VL irradiation. Although it has been reported that the light-excited HA could eject hydrated electrons (e_{aq}^-) into the solution [30], the quantum yield of the generated e_{aq}^- seemed too low to destroy the BPA effectively. Besides, due to the low degradation rate in the two systems, it also ruled out the possibility that the $^3HA^*$ could remove BPA via energy/electron or hydrogen transfer. Surprisingly, when the light was turned on, the PMS/HA/VL system displayed a marvelous enhancement towards BPA degradation, with the degradation rate of BPA reached 95.4% within 30 min. Additionally, after studying the reaction dynamics, the degradation data were found to be well fitted the pseudo-first-order reaction kinetics mode (Fig. 1b). The reaction rate constant of the PMS/HA/VL system was calculated as k = 0.10033 min^{-1}, which was 18.0, 26.3 and 30.8 times higher than that of PMS/VL (k = 0.00558 min^{-1}), PMS/HA/dark (k = 0.00382 min^{-1}), and HA/VL (k = 0.00326 min^{-1}) systems, respectively. These results indicated that the addition of HA could significantly promote the degradation of BPA by PMS under VL irradiation. Compared with other reported VL photocatalytic oxidation and/or PMS oxidation for BPA degradation (Table S1). The PMS/HA/VL system exhibited a relatively rapid BPA degradation or high degradation efficiency. More importantly, the use of HA as the activator of PMS could present a simple and economic reaction process, since HA could be get easily from the nature environment without the complex preparation process.

3.2. HA degradation in PMS/VL system

The concentration and structure change of HA during the reaction process were also explored. To preclude the interference of BPA on the measurement of HA concentration, this part experiments were conducted in the ultrapure water without BPA, and UV_{254} was used to indicate HA concentration. As shown in Fig. 2a, a remarkable reduction was observed for the concentration of HA as measured in UV_{254} (78%) within 30 min. Additionally, $SUVA_{254}$, which is often regarded as an index of the aromaticity of NOM, also decreased substantially with the reduction rate of 70.4%. These results indicated that HA could be effectively degraded by PMS under VL irradiation, and the aromatic components of HA were destroyed in this process. Then, HPSEC/UV was conducted to analyze the molecular weight change of HA before and after reaction in the PMS/VL system. As shown in Fig. 2b, the chromatogram of the non-oxidized HA presented four distinct peaks at about tR = 14, 16, 17 and 18.5 min. As the molecular size of the components is inversely proportional to the retention time, the peak at tR = 14 min can be ascribed to the high molecular weight components which is generally assigned to aromatic components [31]. The other three peaks can be classified as small molecules derived from the division of the high molecular weight components, and the corresponding

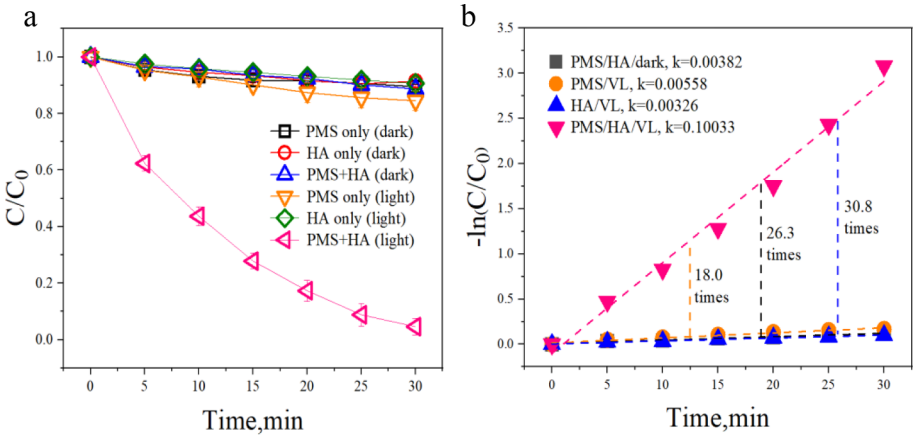

Fig. 1. (a) BPA degradation under different systems; (b) kinetics liner fitting curves. Experimental conditions: [PMS] = 1 mM, HA = 2 mg/L, [BPA] = 10 mg/L, [initial pH] = 4, T = 25 °C.

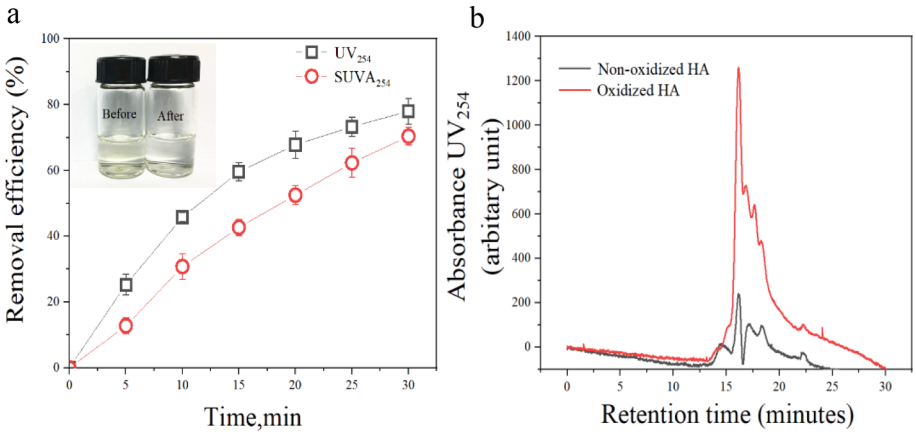

Fig. 2. (a) UV_{254} and SUV_{254} removal efficiencies; and (b) HPSEC/UV chromatograms of HA before and after oxidation in the PMS/VL system. Experimental conditions: [PMS] = 1 mM, [HA] = 2 mg/L, [initial pH] = 4, T = 25 °C. Inlet photo is about the color of solution sample before and after reaction.

molecular weight of the three peaks decreased gradually with the retention time. However, compared with non-oxidized HA, the oxidized HA exhibited a very weak peak at tR = 14 min, but three strong peaks at tR = 16, 17.5, 18.5 min, indicating that the high molecular weight of HA has been converted to the low molecular weight components.

In addition, 3D-EEM fluorescence spectra was employed to reflect the changes of organic pollutants in the PMS/HA/VL system, since it was a sensitive, simple and nondestructive analytical technique which were commonly used to analyze the dissolved organic matter (DOM) [32]. The mapping of the raw solution of BPA (10 mg/L) and HA (2 mg/L), and the solution in PMS/HA/VL system collected at 0 min, dark adsorption for 30 min, light irradiation for 10 min and 30 min were presented in Fig. 3. As shown in Fig. 3a, BPA has two excitation peaks (225 nm and 280 nm) and a single emission peak (310 nm), which could be attributed to the protein-like properties [33], while HA had only one distinct peak at excitation/emission wavelengths (Ex/Em) of 250–290/410–530 nm (Fig. 3b), which could be assigned to fulvic acid [34]. When PMS and HA were spiked into the BPA solution, the characteristic peak of HA changed, two excitation peaks (225–240 nm, 260–290 nm) and a single emission peak (380–420 nm) were observed (Fig. 3c). After 30 min of dark reaction, the fluorescence intensity of HA decreased to some extent, while the fluorescence intensity of protein-like substances was still strong (Fig. 3d). However, when VL was switched on, the fluorescence intensity of the characteristic peaks of both BPA and HA exhibited a distinct reduction after 10 min of reaction (Fig. 3e), and almost disappeared after 30 min of reaction (Fig. 3f). This indicated that both BPA and HA could be effectively oxidized in the PMS/HA/VL system, and the macromolecules like aromatic compounds were fractured and transformed into small molecular like carboxyl, carbonyl, hydroxyl and so on.

3.3. Catalytic oxidation mechanism

To identify the reactive species generated in the PMS/HA/VL system, the radical quenching experiments were conducted using a series of scavengers. Generally, $SO_4^{\cdot -}$ and ·OH are considered as common oxidative species in PMS oxidation processes, they are usually confirmed by MeOH and TBA because of the different rate constants of them with the two radicals (MeOH: 1.2–2.8 × 10^9 M^{-1} s^{-1} for $SO_4^{\cdot -}$ and 1.6–7.7 × 10^7 M^{-1} s^{-1} for ·OH, TBA: 4.0–9.1 × 10^5 M^{-1} s^{-1} for $SO_4^{\cdot -}$ and 3.8–7.6 × 10^8 M^{-1} s^{-1} for ·OH) [35]. If $SO_4^{\cdot -}$ or ·OH was the major oxidizing species, the BPA degradation would be completely inhibited after the addition of MeOH (1 M) and TBA (1 M). However, the degradation rate of BPA was only reduced by 26.6% and 18.2% compared to the control group, respectively (Fig. 4a), indicating that both $SO_4^{\cdot -}$ and ·OH were not the primary reactive species responsible for BPA degradation. The previous studies have reported that as a natural photosensitizer, the VL excited HA could react with dissolved oxygen to generate $O_2^{\cdot -}$ [36]. However, the BPA degradation was barely affected after purging sufficient N_2 to the reaction system, which ruling out the contribution of $O_2^{\cdot -}$ to BPA degradation. Recently, many studies have demonstrated that the PMS direct oxidation and singlet oxygen ($^1O_2$) oxidation could be considered as the dominating oxidation mechanisms in PMS activation processes [37,38]. Nevertheless, Fig. 1a has shown that the degradation rate of BPA was negligible by PMS direct oxidation. Therefore, it can be speculated that $^1O_2$ might be involved in the degradation of BPA.

Furfuryl alcohol (FFA) was generally regarded as a unique scavenger for $^1O_2$ [39]. However, a previous study demonstrated that FFA might react with PMS directly, and thus might not be able to certify the quenching effect toward $^1O_2$ [40]. Based on this consideration, the PMS decomposition experiments were conducted. As shown in Fig. 4b, in the absence of FFA, the residual PMS dosage was 0.48 mM in the PMS (1 mM)/HA/VL system after 30 min of reaction, and the BPA decomposition rate was 95.4%, indicating that there was 0.52 mM PMS involved in producing the reactive species in the system. When FFA (20 mM) was introduced into the PMS (1 mM)/VL system, the PMS was only consumed by 0.32 mM, namely there was 0.68 mM PMS still remained in the solution after 30 min reaction. While, when the same amount of FFA (20 mM) was added to the PMS (1 mM)/HA/VL system, the residual PMS was measured to be only 0.15 mM, indicating that 20 mM FFA could not consume overmuch PMS, thus addition of 20 mM FFA could not influence the ROS generation. Furthermore, it should be noted that the reaction between FFA and PMS was relatively slow that the FFA concentration was almost unchanged throughout the reaction process (Fig. 4c). However, in this situation, the BPA degradation was almost inhibited, manifesting that reactive oxygen species (mainly $^1O_2$) has been quenched by FFA, thus FFA could be used as the scavenger for $^1O_2$ in this study. As shown in Fig. 4a, FFA exhibited a strong inhibitory effect on PMS/HA/VL system, even at a concentration of 1 mM, the BPA degradation rate was decreased by 23.8%. With increasing the FFA concentration to 10 mM, the oxidation of BPA further decreased to 13.8%, and almost completely terminated when FFA concentration increased to 20 mM. Notably, although FFA is also an efficient scavenger for $SO_4^{\cdot -}$ and ·OH, both $SO_4^{\cdot -}$ and ·OH were not the primary reactive species responsible for BPA oxidation in this study (Fig. 4a). Hence, the above results showed that $^1O_2$ was the primary reactive species generated in PMS/HA/VL system responsible for BPA degradation.

To further confirm the existence of $^1O_2$ in PMS/HA/VL system, the HPLC/APCI-QqQMS technique was employed, which was according to the fact that DPA (a chemical probe) could react with $^1O_2$ to produce the indicative endoperoxide ($DPAO_2$) [25]. As shown in Fig. S3a, the characteristic peak of $DPAO_2$ appeared in the DPA/HA/PMS/VL

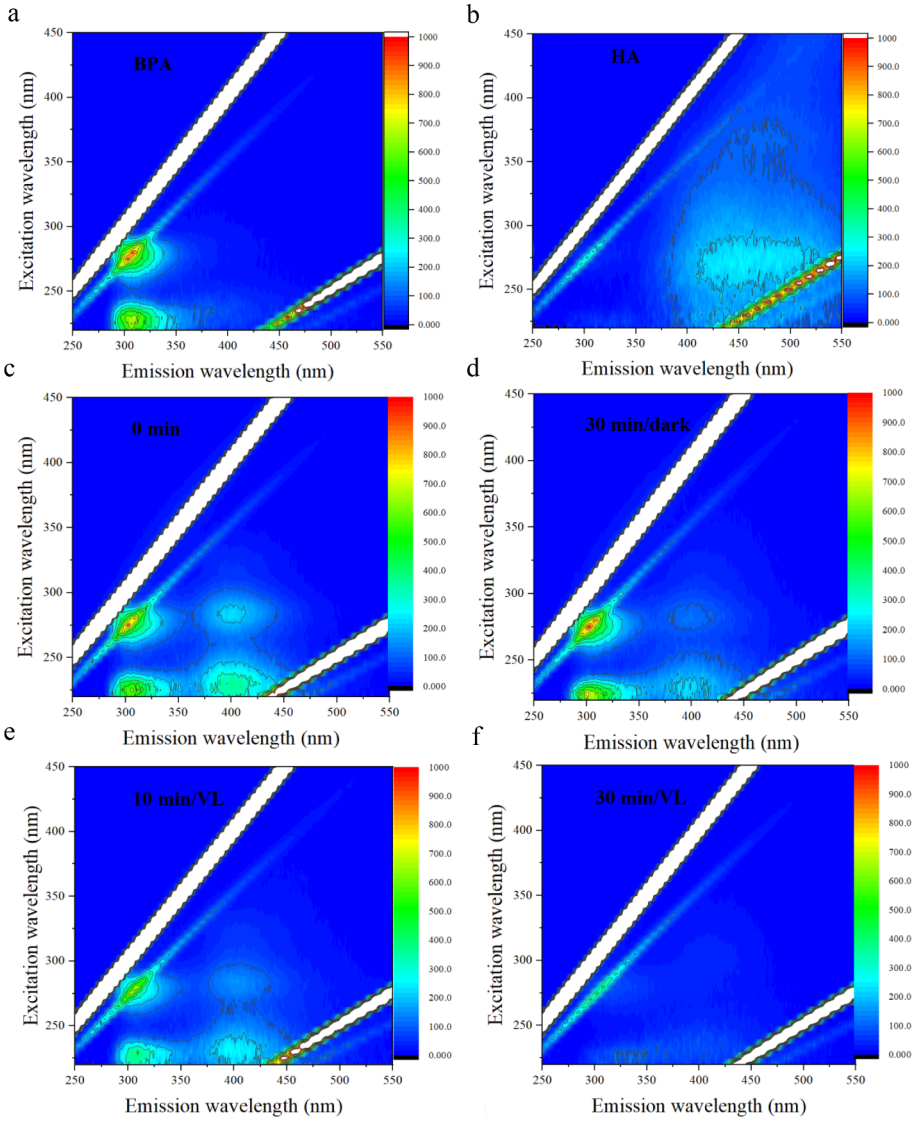

Fig. 3. 3D-EEMs spectra of (a) original BPA solution (10 mg/L); (b) HA (2 mg/L); (c) PMS/HA/BPA system at 0 min, (d) 30 min in dark, (e) 10 min in VL, and (f) 30 min in VL. Experimental conditions: [PMS] = 1 mM, HA = 2 mg/L, [BPA] = 10 mg/L, [initial pH] = 4, T = 25 °C.

system, and the peak intensity was shown to be enhanced with increasing the concentration of PMS (from 0.1 to 1 mM) in the presence of 2 mg/L HA. Comparatively, both the DPA/PMS group and the DPA blank group presented a weak signal of $DPAO_2$, which might be due to the low quantum yield of $^1O_2$ from the self-decomposition of PMS and the impurity of DPA chemical, respectively. It should be noted that these two peaks were so weak that they were almost invisible compared to the peaks in Fig. S3a, so they were presented separately in Fig. S3b. The above results further verified the involvement of $^1O_2$ in the PMS/HA/VL system.

Additionally, EPR experiments were conducted to identify the reactive species generated in the PMS/HA/VL system by using DMPO and TMP as the spin trap agents. It was clearly seen that the characteristic peaks of DMPO-·OH adducts and DMPO-$SO_4^{\cdot -}$ adducts were both detected for the PMS/HA/VL system (Fig. 4d). Besides, a typical 1:1:1 triplet signal characteristic peak of TMP-$^1O_2$ were also observed (Fig. 4e), and the intensity of the peaks became stronger with the reaction time increased (Fig. 4f). The EPR experimental results were consistent with the results of quenching experiments and further confirmed the appearance of reactive species (·OH, $SO_4^{\cdot -}$ and $^1O_2$) in the PMS/HA/VL system.

HA is the mixture of naturally occurring organic polyelectrolytes which contains a variety of functional groups, and the chemical composition differs in different molecular size fractions of HA. Namely, there is significant variation in terms of the quantity and properties of the functional groups in different molecular size fractions of HA [41]. Thus, in order to explore which component in HA contributed the most to the BPA degradation, HA was fractionalized into four molecular size classes with molecular size of < 5 kD, 5–30 kD, 30–100 kD, and > 100 kD, respectively. As displayed in Fig. 5a, $HA_{5–30\ kD}$ promoted the fastest degradation of BPA compared with other molecular size fractions. Within 30 min, BPA could be completely removed in the PMS/$HA_{5–30kD}$/VL system. Meanwhile, the PMS/$HA_{30–100kD}$/VL, PMS/$HA_{<5kD}$/VL, PMS/$HA_{>100\ kD}$/VL systems exhibited 72.2%, 14.4% and 8.2% of BPA removal, respectively. The BPA removal efficiency by PMS/$HA_{5–30\ kD}$/VL system was 1.39-fold, 6.94-fold and 12.2-fold higher than that of PMS/$HA_{30–100kD}$/VL, PMS/$HA_{<5kD}$/VL and PMS/$HA_{>100\ kD}$/VL systems, respectively, indicating that $HA_{5–30\ kD}$ play a major role in BPA degradation in PMS/HA/VL system.

Then the FT-IR and 3D-EEMs spectra were employed to characterize the composition of functional groups and structural properties of different molecular size fractions of HA. In the FT-IR spectra (Fig. 5b), the broad band at 3700–3200 cm^{-1} could be ascribed to the phenolic O–H stretching, and the peak at 1600 cm^{-1} represented the C=O bond or

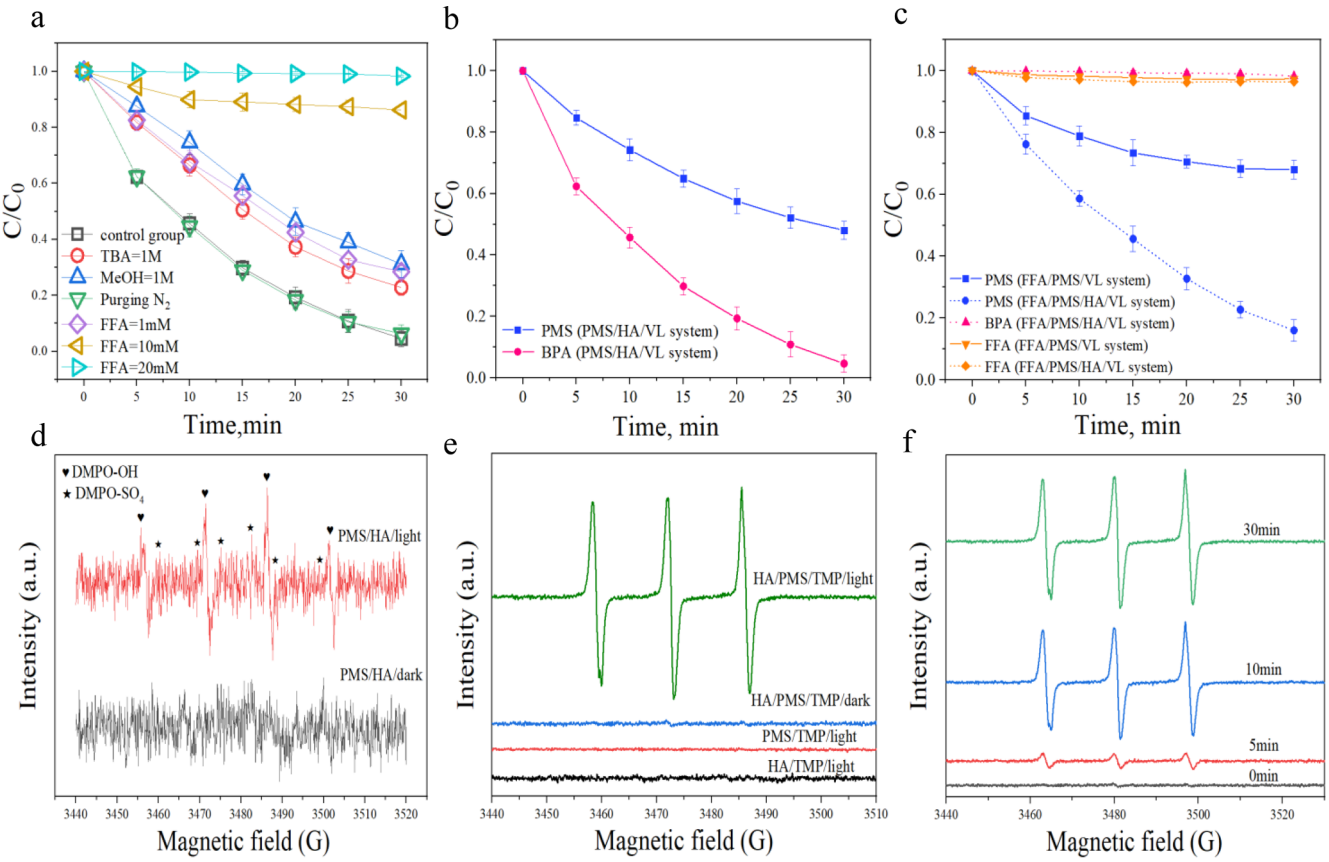

Fig. 4. (a) Effect of different quenchers on BPA degradation in the PMS/HA/VL system; (b) PMS and BPA decomposition in the absence of FFA; (c) PMS, BPA and FFA decomposition in the presence of FFA (20 mM); (d) DMPO and (e) TEMP spin-trapping EPR spectra of different systems; and (f) $^1O_2$ production in HA/PMS/TMP/VL system in different reaction times. Experimental conditions: [PMS] = 1 mM, [BPA] = 10 mg/L, [HA] = 2 mg/L, [TBA] = 1 mM, [MeOH] = 1 mM, [FFA] = 1–20 mM, [DMPO] = 10 mM, [TEMP] = 20 mM, [initial pH] = 4, T = 25 °C.

aromatic ring C═C–C bond, which can be classified as the stretching of conjugated ketones and quinones [42]. As shown in Fig. 5b, the peak strength of phenolic O–H in $HA_{5–30\ kD}$ was much higher than that in other molecular size fractions of HA, indicating that $HA_{5–30\ kD}$ owned the most abundant phenolic groups among the four molecular size fractions of HA. However, there was no much difference of the conjugated ketones and quinones peaks among the four fractions, though the peak in $HA_{5–30\ kD}$ was slightly higher than that of the other three ones. Besides, compared with original $HA_{5–30\ kD}$, the two characteristic peaks of phenolic groups and conjugated ketones/quinone groups in oxidized $HA_{5–30\ kD}$ were found to be decreased obviously. Combined with the results of Fig. 5a, it could thus be speculated that the phenolic groups and conjugated ketones/quinone groups of HA might participate in the reaction process and make the major contribution to the BPA degradation in the PMS/HA/VL system.

The previous study has reported that the extent of aromatic structures in NOM can be determined by the fluorescence index, which is defined as the ratio of fluorescence emission intensity at wavelength of 450 nm to that at 500 nm under the excitation wavelength of 370 nm [43]. Fig. 5c-f present the 3D-EEMs spectra of different molecular size fractions of HA. In this work, the fluorescence index value of $HA_{5–30\ kD}$ was 1.14, which was higher than that of $HA_{30–100\ kD}$ and the mother HA solution (0.82 and 1.08, respectively), indicating that $HA_{5–30\ kD}$ contained more aromatic constituents than other molecular size fractions of HA. Additionally, Klapper et al. had found that there was a positive correlation between the electron donating capability of HA and the fluorescence index [44]. Accordingly, the electron-donating ability of $HA_{5–30\ kD}$ would also be stronger and the $HA_{5–30\ kD}$ should be able to favor the BPA degradation in the PMS/HA/VL system. For example, the degradation rate of BPA could reach almost 100% within 20 min in the PMS/$HA_{5–30\ kD}$/VL system (Fig. 5a), while this value was 95.4% (Fig. 1a) and 77.6% (Fig. 5a) in the PMS/HA/VL and PMS/$HA_{30–100\ kD}$/VL systems after 30 min of reaction, respectively. These results indicated that the BPA degradation was positively correlated with the aromaticity degree of HA and its electron-donating capacity. It has been reported that phenolic groups contribute to the electron-donating capacity of HA [45]. Combining with the results of above, it could be speculated that the BPA degradation also had a positive relationship with the content of phenolic groups in HA.

The fluorescence peak at Ex/Em = 305 nm/540 nm of $HA_{5–30\ kD}$ could be ascribed to the fulvic acid fraction of HA [46]. It was reported that the quinone groups accounted for 50% of the fulvic acid-like fluorescence region and played a dominant role in electrons transferring [47]. As can be seen in Fig. 5d, $HA_{5–30\ kD}$ owned the stronger peak at Ex/Em = 305 nm/540 nm than other molecular size fractions of HA, indicating that $HA_{5–30\ kD}$ owned the most quinone groups compared with other molecular size fractions of HA, which was consistent with the results of FT-IR analysis (Fig. 5b). The previous study had reported that as an electron-shuttle, quinone could enhance the electron-transfer between HA and electron acceptors (i.e., oxidants) [48]. Thus, in this study, since PMS was one of the oxidants, we proposed that the enhanced degradation of BPA in PMS/HA/VL system was also related to the electron shuttling effects brought by quinone groups of HA, which accelerated the electron transfer between HA and PMS.

Based on the above analysis, the mechanism of PMS activation by HA under VL irradiation for the degradation of organic pollutants was proposed and shown in Fig. 6. Firstly, under VL irradiation, HA in aqueous solution (HA_{aq}) will be excited and eject the solvated electrons

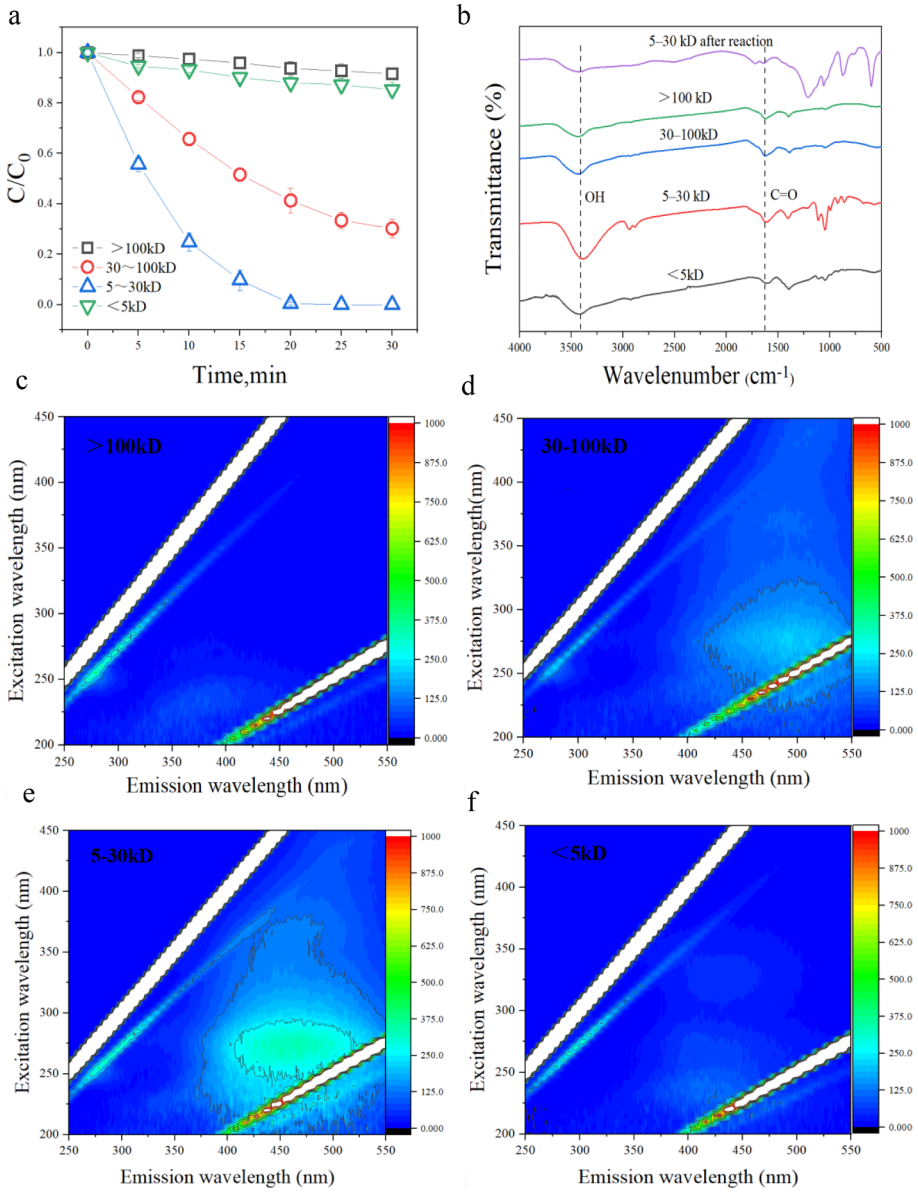

Fig. 5. (a) BPA degradation in PMS/HA/VL system with different molecular sizes of HA; (b) FT-IR spectra of different molecular sizes of HA; 3D-EEMs of different size fractions of HA: (c) $HA_{>100kD}$, (d) $HA_{30\text{-}100kD}$, (e) $HA_{5\text{-}30kD}$, (f) $HA_{<5kD}$. Experimental conditions: [PMS] = 1 mM, HA = 2 mg/L, [BPA] = 10 mg/L, [initial pH] = 4, T = 25 °C.

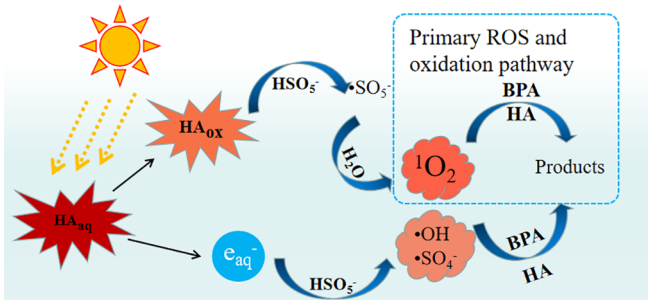

Fig. 6. Proposed schematic diagram of visible-light-excited humic acid for PMS activation to degrade BPA.

(e_{aq}^-) to the solution, and then became an oxidation state HA (HA_{ox}) (Eqs. (1) and (2)) [49]. Based on the analysis of FT-IR and 3D-EEMs, the e_{aq}^- came mainly from the aromatic constituents of HA, in this study, it mainly referred to the phenolic groups. Then, as the electron shuttles, the quinone moieties would accelerate the electron-transfer between HA and PMS. As the electron acceptor, PMS could react with e_{aq}^- to generate $SO_4^{\cdot -}$ and ·OH (Eq. (3)). Besides, PMS could also react with HA_{ox} to generate $SO_5^{\cdot -}$ (Eq. (4)), which was responsible for the production of $^1O_2$ (Eq. (5)). Finally, all the generated reactive species made their contributions to the degradation of organic pollutant in the solution (Eq. (6)).

$$HA_{aq} \xrightarrow{h\nu} HA_{aq}* \quad (1)$$

$$HA_{aq}* \rightarrow HA_{ox} + e_{aq}^- \quad (2)$$

$$e_{aq}^- + HSO_5^- \rightarrow SO_4^{\cdot -} + \cdot OH \quad (3)$$

$$HA_{ox} + HSO_5^- \rightarrow HA_{aq} + SO_5^{\cdot -} + H^+ \quad (4)$$

$$2SO_5^{\cdot -} + H_2O \rightarrow 1.5\ ^1O_2 + 2HSO_4^- \quad (5)$$

$$^1O_2 + \cdot OH + SO_4^{\cdot -} + BPA/HA_{aq} \rightarrow \text{products} \quad (6)$$

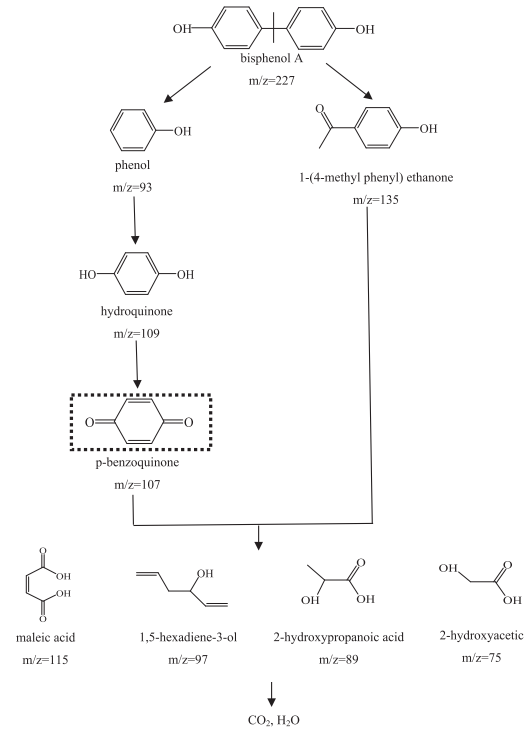

Fig. 7. Proposed degradation pathways of BPA in PMS/HA/VL system.

3.4. Degradation pathways of BPA in the PMS/HA/VL system

DOC measurements showed that DOC removal efficiency in PMS/HA/VL system was 57.6% after 60 min reaction (Fig. S4), and there was still 42.4% of DOC remaining in the system. The incompletely mineralized BPA would be converted to other oxidation intermediates, which might exert higher toxicity than the parent compound. Based on this, UPLC/MS/MS was employed to characterize the oxidation intermediates of BPA. Details of the oxidation products of BPA and MS/MS fragmentation information were shown in Fig. S5. According to these oxidation products, the probable degradation pathways were proposed in Fig. 7. Since the electron-donating hydroxyl group could enhance the electron density of each aromatic ring, the bond which linking two aromatic rings in BPA was more fragile to be attacked [50]. Thus, a β-scission of isopropyl would take place between two phenyl groups of BPA firstly, which leading to the generation of phenol (m/z = 93) and 1-(4-methyl phenyl) ethanone (m/z = 135). The phenol would be further oxidized to hydroquinone (m/z = 109), which is not a very stable chemical substance and subsequently degraded to p-benzoquinone (m/z = 107) subsequently. Notably, p-benzoquinone (m/z = 107) presented in the pathway could not be detected as it is not able to be ionized [51]. Then these oxidation products would be further attacked to generate maleic acid (m/z = 115), 1,5-hexadiene-3-ol (m/z = 97), 2-hydroxypropanoic acid (m/z = 89) and 2-hydroxyacetic (m/z = 75).

3.5. Effect of operating parameters on BPA degradation

As displayed in Fig. 8a, with HA concentrations ranged from 0.5 to 2 mg/L, the degradation rate of BPA increased rapidly as compared to PMS/VL system. For the concentrations of HA at 0, 0.5, 1 and 2.0 mg/L, the degradation rates were 15.5%, 63.3%, 70.18% and 95.4%, respectively. However, with the HA concentration further increased from 5 to 10 mg/L, the degradation efficiency of BPA increased marginally, which was probably owing to the fact that the amount of PMS in the system was limited, and there was not enough PMS to react with the excess HA to produce the reactive species. Besides, though the excited HA could also oxidize the pollutant by ejecting the e_{aq}^- into the solution, the quantum yield seemed to be too low to oxidize the pollutants efficiently, and the overmuch HA might play a role of light screens to reduce the light reception in the system [23].

Fig. 8b displays the effect of PMS concentration on BPA degradation. With the PMS concentration increased, the degradation efficiency was remarkably promoted. For example, when PMS concentration was 0.1 mM, the degradation rate of BPA was only 48.8% within 30 min. When PMS concentration increased to 2 mM, the BPA could be degraded nearly 100% within 20 min, and it only took 15 min to completely remove the BPA from the system at PMS concentration of 5 mM. This can be attributed to that the high PMS concentration would have more opportunities to contact with HA to generate more ROS, leading to the promotion of BPA degradation. Further increasing PMS concentration to 10 mM, the BPA degradation rate was no longer increased, on the contrary, there was a slight inhibition observed for BPA degradation compared to that of 2 mM and 5 mM PMS. This could be probably ascribed to the fact that the amount of HA in the system was not enough to react with the excess PMS, and the self-scavenging of $SO_4^{\cdot -}$ radicals might also reduce the amount of ROS [52], thus retarding the degradation of BPA.

As shown in Fig. 8c, when the initial BPA concentration was 5 mg/L, BPA could be completely removed within 30 min. As BPA concentration increased from 5 mg/L to 50 mg/L, the degradation efficiency was decreased to 41.4%. Thus, there was a negative correlation between the degradation rate and initial BPA concentration, indicating that more reaction time or more PMS was needed as BPA concentration in the system increased.

Fig. 8d depicts the influence of initial pH on BPA degradation in the PMS/HA/VL system. The natural pH of the system is 4 without any adjustment. As shown in Fig. 8d, the BPA degradation under acidic conditions was faster than that of the alkaline conditions. The reaction rate constant was changed from 0.1299 min^{-1} to 0.01125 min^{-1} as the initial pH of the system varied from 3 to 9. This could be ascribed to the fact that PMS existed as anion over a wide range of pH (i.e., pKa_1 = 0.4 and pKa_2 = 9.3) [53], while most HA could be protonated and positively charged at acidic pH, thus leading to an enhanced interaction probability between HA and PMS due to the electrostatic attraction, which could facilitate subsequent reaction. On the contrary, since HA contained many acidic functional groups, it would undergo deprotonation reaction under alkaline conditions and be negatively charged. Therefore, on account of the negative-negative electrostatic repulsion, the contact opportunities between HA and PMS under alkaline conditions were not as much as under the acidic conditions [20], resulting in the slow BPA degradation.

3.6. Effect of water matrices on BPA degradation in PMS/HA/VL system

It was reported that the inorganic anions in natural waters can scavenge radicals, thus resulting in the decreased oxidation ability in the radical-based oxidation process [54]. However, the non-radical oxidation process was regarded to avoid this problem. Since we had proved that the radical and nonradical pathways were co-existed in the PMS/HA/VL system, it was necessary to investigate the effect of various anions on BPA degradation in the PMS/HA/VL system. As displayed in Fig. 9, Cl^- slightly boosted the BPA degradation. It is well-known that Cl^- can react with ·OH/$SO_4^{\cdot -}$ to generate reactive chlorine species including Cl·, Cl_2, $Cl_2^{\cdot -}$, $ClOH^{\cdot -}$, and HOCl [55]. These reactive chlorine species have high reactivity for the phenolic compounds. Hence, it was likely that reactive chlorine species accounted for the slight enhanced BPA removal. However, HPO_4^{2-} and HCO_3^- displayed a slightly inhibition to the BPA degradation, this could be ascribed to the fact that both HPO_4^{2-} and HCO_3^- could scavenge the radicals ($SO_4^{\cdot -}$ and ·OH) of the system [56,57], thereby restraining the BPA degradation. Additionally, NO_3^- exerted negligible effect on BPA degradation, which might be due to the low rate constant between NO_3^-

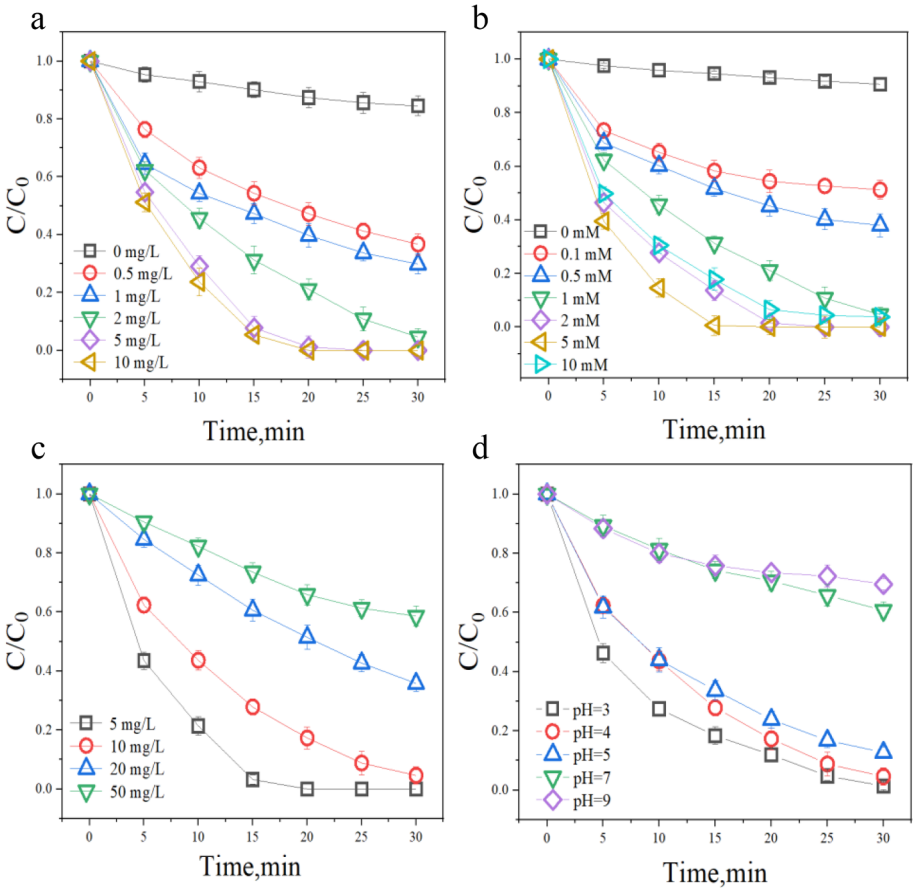

Fig. 8. Effect of operating parameters on BPA degradation in PMS/HA/VL system. (a) HA dosage; (b) PMS concentration; (c) BPA concentration; (d) initial pH. Experimental conditions: [HA] = 0.5–10 mg/L, [PMS] = 0.1–5 mM, [BPA] = 5–50 mg/L, [initial pH] = 3–9, T = 25 °C.

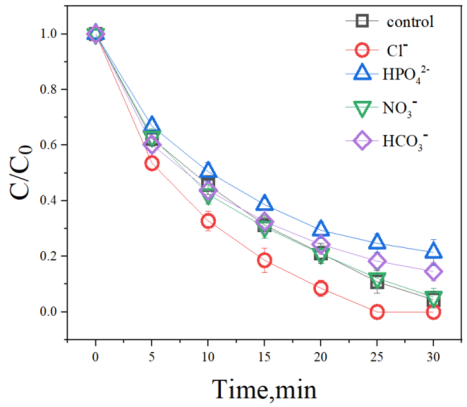

Fig. 9. Effect of water matrices on BPA degradation in PMS/HA/VL system. Experimental conditions: $[Cl^-]$ = $[HPO_4^{2-}]$ = $[NO_3^-]$ = $[HCO_3^-]$ = 10 mM, [PMS] = 1 mM, [HA] = 2 mg/L, [BPA] = 10 mg/L, T = 25 °C.

with $SO_4^{\cdot -}$ [58]. The above results indicated that the oxidation capacity of the PMS/HA/VL system would not be greatly affected by the water matrices, which ensuring the practical applicability of the system.

4. Conclusions

Overall, a new PMS activation method which employed VL excited HA as activator for the removal of BPA was developed in this work. The results indicated that the introduction of HA to the PMS/VL system could significantly promote BPA degradation. In this process, the original structure of HA was damaged and transformed to the low weight molecular fractions. The quenching tests and EPR characterization indicated that $SO_4^{\cdot -}$, ·OH and $^1O_2$ were all generated in the PMS/HA/VL system, and $^1O_2$ played the dominant role to the BPA degradation. Additionally, the BPA degradation was positively correlated with the aromaticity degree of HA, in which the phenolic groups and the quinone moieties in HA promoted the electron-donating and electron-transfer ability of HA, respectively. Besides, the inorganic anions in waters would not make a great influence on BPA degradation, which indicated the excellent practical applicability of the system. Since HA is ubiquitous in nature environment, this work may provide a new perspective for the in situ remediation of water by incorporating AOPs.

Declaration of Competing Interest

The authors declare that they have no known competing financial interests or personal relationships that could have appeared to influence the work reported in this paper.

Acknowledgments

This work was supported by the National Natural Science Foundation of China (NO. 50808052 and 51978232). The Natural Science Foundation of Hebei Province (No. E2019202012), and the Natural Science Foundation of Tianjin (No. 19JCJQJC63000).

Appendix A. Supplementary data

Supplementary data to this article can be found online at https://doi.org/10.1016/j.cej.2020.125853.

References

[1] G.P. Anipsitakis, D.D. Dionysiou, Degradation of organic contaminants in water with sulfate radicals generated by the conjunction of peroxymonosulfate with cobalt, Environ Sci. Technol. 37 (20) (2003) 4790–4797.

[2] M.G. Antoniou, A.A. de la Cruz, D.D. Dionysiou, Degradation of microcystin-LR using sulfate radicals generated through photolysis, thermolysis and e-transfer mechanisms, Appl. Catal. B-Environ. 96 (2010) 290–298.

[3] J. Liu, J. Zhou, Z. Ding, Z. Zhao, X. Xu, Z. Fang, Ultrasound irritation enhanced heterogeneous activation of peroxymonosulfate with Fe_3O_4 for degradation of azo dye, Ultrason. Sonochem. 34 (2017) 953–959.

[4] W.H. Chu, D.M. Li, N.Y. Gao, M.R. Templeton, C.Q. Tan, Y.Q. Gao, The control of emerging haloacetamide DBP precursors with UV/persulfate treatment, Water Res. 72 (2015) 340–348.

[5] X.G. Duan, Z.M. Ao, H.Q. Sun, L. Zhou, G.X. Wang, S.B. Wang, Insights into N-doping in single-walled carbon nanotubes for enhanced activation of superoxides: a mechanistic study, Chem. Commun. 51 (2015) 15249–15252.

[6] Y. Feng, D.L. Wu, Y. Deng, T. Zhang, K.M. Shih, Sulfate radical-mediated degradation of sulfadiazine by $CuFeO_2$ rhombohedral crystal-catalyzed peroxymonosulfate: synergistic effects and mechanism, Environ Sci. Technol. 50 (2016) 3119–3127.

[7] G.P. Anipsitakis, D.D. Dionysiou, Radical generation by the interaction of transition metals with common oxidants, Environ. Sci. Technol. 38 (2004) 3705–3712.

[8] O.S. Furman, A.L. Teel, R.J. Watts, Mechanism of base activation of persulfate, Environ Sci. Technol. 44 (2010) 6423–6428.

[9] J.L. Wang, S.Z. Wang, Activation of persulfate (PS) and peroxymonosulfate (PMS) and application for the degradation of emerging contaminants, Chem. Eng. J. 334 (2018) 1502–1517.

[10] Y.-H. Guan, J. Ma, X.-C. Li, J.-Y. Fang, L.-Y. Chen, Influence of pH on the formation of sulfate and hydroxyl radicals in the UV/peroxymonosulfate system, Environ Sci. Technol. 45 (2015) 9308–9314.

[11] G.P. Anipsitakis, D.D. Dionysiou, Transition metal/UV-based advanced oxidation technologies for water decontamination, Appl. Catal. B: Environ. 54 (2004) 155–163.

[12] Y.S. Jo, C.Y. Kim, G.H. Moon, J.S. Lee, T.C. An, W.Y. Choi, Activation of peroxymonosulfate on visible light irradiated TiO2 via a charge transfer complex path, Chem. Eng. J. 346 (2018) 249–257.

[13] Y. Liu, H.G. Guo, Y.L. Zhang, W.H. Tang, X. Cheng, H.W. Liu, Activation of peroxymonosulfate by $BiVO_4$ under visible light for degradation of Rhodamine B, Chem. Phys. Lett. 653 (2016) 101–107.

[14] K.X. Zhu, J.H. Wang, Y.J. Wang, C.Z. Jin, A.S. Ganeshraja, Visible-light-induced photocatalysis and peroxymonosulfate activation over $ZnFe_2O_4$ fine nanoparticles for degradation of Orange II, Catal. Sci. Technol. 6 (2016) 2296–2304.

[15] K. Ghosh, M. Schnitzer, Macromolecular structure of humic substances, Soil Sci. 129 (1980) 266–276.

[16] N. Senesi, F.R. Rizzi, P. Dellino, P. Acquafredda, Fractal humic acids in aqueous suspensions at various concentrations, ionic strengths, and pH values, Colloid Surf A 127 (1997) 57–68.

[17] R.A. Alvarez-Puebla, C. Valenzuela-Calahorro, J. Garrido, X.T. Zhou, Theoretical study on fulvic acid structure, conformation and aggregation a molecular modelling approach, Sci. Total Environ. 358 (2006) 243–254.

[18] Y. Chen, C. Hu, X.X. Hu, J.H. Qu, Indirect photodegradation of amine drugs in aqueous solution under simulated sunlight, Environ Sci. Technol. 43 (2009) 2760–2765.

[19] Y.H. Pan, S. Garg, T.D. Waite, X. Yang, Copper inhibition of triplet-induced reactions involving natural organic matter, Environ. Sci. Technol. 52 (2018) 2742–2750.

[20] Y.M. Cho, W.Y. Choi, Visible light-induced reactions of humic acids on TiO_2, J. Photochem. Photobiol., A 148 (2002) 129–135.

[21] J.Y. Yao, R.J. Qu, W.X. Hao, V.K. Sharma, A. Shad, A.A. Dar, Z.Y. Wang, Visible light and fulvic acid assisted generation of Mn(III) to oxidize bisphenol A: the effect of tetrabromobisphenol A, Water Res. 169 (2020) 115273.

[22] X.H. Wang, S.Y. Wang, R.J. Qu, J.L. Ge, Z.Y. Wang, C. Cheng, Enhanced removal of chlorophene and 17β-estradiol by Mn(III) in a mixture solution with humic acid: investigation of reaction kinetics and formation of co-oligomerization products, Environ. Sci. Technol. 52 (2018) 13222–13230.

[23] C.X. Guo, C.J. Zhang, Z.Y. Sun, X.Y. Zhao, Q. Zhou, M.R. Hoffmann, Synergistic impact of humic acid on the photo-reductive decomposition of perfluorooctanoic acid, Chem. Eng. J. 360 (2019) 1101–1110.

[24] F.M. Dunnivant, R.P. Schwarzenbach, D.L. Macalady, Reduction of substituted nitrobenzenes in aqueous-solutions containing natural organic-matter, Environ Sci. Technol. 26 (1992) 2133–2141.

[25] S. Miyamoto, G.R. Martinez, M.H.G. Medeiros, P. Di Mascio, Singlet molecular oxygen generated from lipid hydroperoxides by the russell mechanism: Studies using ^{18}O-labeled linoleic acid hydroperoxide and monomol light emission measurements, J. Am. Chem. Soc. 125 (2003) 6172–6179.

[26] M. Andersson, L. Osterlund, S. Ljungstrom, A. Palmqvist, Preparation of nanosize anatase and rutile TiO_2 by hydrothermal treatment of microemulsions and their activity for photocatalytic wet oxidation of phenol, J. Phys. Chem. B 106 (2002) 10674–10679.

[27] J.A. Khan, X. He, N.S. Shah, H.M. Khan, E. Hapeshi, D. Fatta-Kassinos, D.D. Dionysiou, Kinetic and mechanism investigation on the photochemical degradation of atrazine with activated H_2O_2, $S_2O_8^{2-}$ and HSO_5^-, Chem. Eng. J. 252 (2014) 393–403.

[28] Y. Zhou, J. Jiang, Y. Gao, J. Ma, S.Y. Pang, J. Li, X.T. Lu, P.L. Yuan, Activation of peroxymonosulfate by benzoquinone: a novel nonradical oxidation process, Environ. Sci. Technol. 49 (2015) 12941–12950.

[29] G.S. Liu, Y.N. Zhou, J. Teng, J.N. Zhang, S.J. You, Visible-light-driven photocatalytic activation of peroxymonosulfate by $Cu_2(OH)PO_4$ for effective decontamination, Chemosphere 201 (2018) 197–205.

[30] T.E. Thomas-Smith, N.V. Blough, Photoproduction of hydrated electron from constituents of natural waters, Environ Sci. Technol. 35 (2001) 2721–2726.

[31] B. Roshani, N.K.V. Leitner, Effect of persulfate on the oxidation of benzotriazole and humic acid by e-beam irradiation, J. Hazard. Mater. 190 (2011) 403–408.

[32] S. García Ballesteros, M. Costante, R. Vicente, M. Mora, A.M. Amat, A. Arques, L. Carlos, F.S. García Einschlag, Humic-like substances from urban waste as auxiliaries for photo-fenton treatment: a fluorescence EEM-PARAFAC study, Photochem. Photobiol. Sci. 16 (2017) 38–45.

[33] H.R. Yu, H. Liang, F.S. Qu, Z.-S. Han, S.L. Shao, H.Q. Chang, G.B. Li, Impact of dataset diversity on accuracy and sensitivity of parallel factor analysis model of dissolved organic matter fluorescence excitation-emission matrix, Sci. Rep. 5 (2015) 10207.

[34] L.O. Villacorte, Y. Ekowati, T.R. Neu, J.M. Kleijn, H. Winters, G. Amy, J.C. Schippers, M.D. Kennedy, Characterisation of algal organic matter produced by bloom-forming marine and freshwater algae, Water Res. 73 (2015) 216–230.

[35] Y. Zhang, B.J. Wang, X.N. Hu, H.J. Li, Non-activated peroxymonosulfate oxidation of *p*-aminobenzoic acid in the presence of effluent organic matter, Chem. Eng. J. 384 (2020) 123247.

[36] R.M. Dalrymple, A.K. Carfagno, C.M. Sharpless, Correlations between dissolved organic matter optical properties and quantum yields of singlet oxygen and hydrogen peroxide, Environ Sci. Technol. 44 (15) (2010) 5824–5829.

[37] D.G. Li, X.G. Duan, H.Q. Sun, J. Kang, H.Y. Zhang, M.O. Tade, S.B. Wang, Facile synthesis of nitrogen-doped graphene via low-temperature pyrolysis: the effects of precursors and annealing ambience on metal-free catalytic oxidation, Carbon 115 (2017) 649–658.

[38] P. Liang, C. Zhang, X.G. Duan, H.Q. Sun, S.M. Liu, M.O. Tade, S.B. Wang, An insight into metal organic framework derived N-doped graphene for the oxidative degradation of persistent contaminants: formation mechanism and generation of singlet oxygen from peroxymonosulfate, Environ Sci. Nano. 4 (2017) 315–324.

[39] H.M. Xu, W.J. Cooper, J.Y. Jung, W.H. Song, Photosensitized degradation of amoxicillin in natural organic matter isolate solutions, Water Res. 45 (2011) 632–638.

[40] E.T. Yun, J.H. Lee, J. Kim, H.D. Park, J. Lee, Identifying the nonradical mechanism in the peroxymonosulfate activation process: singlet oxygenation versus mediated electron transfer, Environ Sci. Technol. 52 (2018) 7032–7042.

[41] I. Christl, C.J. Milne, D.G. Kinniburgh, R. Kretzschmar, Relating ion binding by fulvic and humic acids to chemical composition and molecular Size. 2. Metal binding, Environ Sci. Technol. 35 (2001) 2512–2517.

[42] X.K. Tian, C. Tian, Y.L. Nie, C. Dai, C. Yang, N. Tian, Z.X. Zhou, Y. Li, Y.X. Wang, Controlled synthesis of dandelion-like $NiCo_2O_4$ microspheres and their catalytic performance for peroxymonosulfate activation in humic acid degradation, Chem. Eng. J. 331 (2018) 144–151.

[43] W. Chen, P. Westerhoff, J.A. Leenheer, K. Booksh, Fluorescence excitation – emission matrix regional integration to quantify spectra for dissolved organic matter, Environ Sci. Technol. 37 (2003) 5701–5710.

[44] L. Klapper, D.M. McKnight, J.R. Fulton, E.L. Blunt-Harris, K.P. Nevin, D.R. Lovley, P.G. Hatcher, Fulvic acid oxidation state detection using fluorescence spectroscopy, Environ Sci. Technol. 36 (2002) 3170–3175.

[45] M. Aeschbacher, D. Vergari, R.P. Schwarzenbach, M. Sander, Electrochemicalanalysis of proton and electron transfer equilibria of the reducible moieties in humic acids, Environ Sci. Technol. 45 (2011) 8385–8394.

[46] J.A. Leenheer, J.P. Croue, Characterizing aquatic dissolved organic matter, Environ Sci. Technol. 37 (2003) 18A–26A.

[47] R.M. Cory, D.M. McKnight, Fluorescence spectroscopy reveals ubiquitous presence of oxidized and reduced quinones in dissolved organic matter, Environ Sci. Technol. 39 (2005) 8142–8149.

[48] E.E. Roden, A. Kappler, I. Bauer, J. Jiang, A. Paul, R. Stoesser, H. Konishi, H.F. Xu, Extracellular electron transfer through microbial reduction of solid-phase humic substances, Nat. Geosci. 3 (2010) 417–421.

[49] R.G. Zepp, A.M. Braun, J. Hoigne, J.A. Leenheer, Photoproduction of hydrated electrons from natural organic solutes in aquatic environments, Environ Sci. Technol. 21 (1987) 485–490.

[50] T. Zhang, Y.B. Ding, H.Q. Tang, Generation of singlet oxygen over Bi(V)/Bi(III) composite and its use for oxidative degradation of organic pollutants, Chem. Eng. J. 264 (2015) 681–689.

[51] Q. Wang, Z. Liu, D. Liu, G. Liu, M. Yang, F. Cui, W. Wang, Ultrathin two-dimensional $BiOBr_xI_{1-x}$ solid solution with rich oxygen vacancies for enhanced visible-light-driven photoactivity in environmental remediation, Appl. Catal. B: Environ. 236 (2018) 222–232.

[52] H.Z. Wang, W.Q. Guo, B.H. Liu, Q.L. Wu, H.C. Luo, Q. Zhao, Q.S. Qi, F. Sseguy, N.Q. Ren, Edge-nitrogenated biochar for efficient peroxydisulfate activation: an electron transfer mechanism, Water Res. 160 (2019) 405–414.

[53] H. Elias, U. Gotz, K.J. Wannowius, Kinetics and mechanism of the oxidation of sulfur(Iv) by peroxomonosulfuric acid anion, Atmos. Environ. 28 (1994) 439–448.

[54] W.L. Wang, Q.Y. Wu, N. Huang, T. Wang, H.Y. Hu, Synergistic effect between UV

and chlorine (UV/chlorine) on the degradation of carbamazepine: influence factors and radical species, Water Res. 98 (2016) 190–198.
[55] J. Moreno-Andres, G. Farinango, L. Romero-Martínez, A. Acevedo-Merino, E. Nebot, Application of persulfate salts for enhancing UV disinfection in marine waters, Water Res. 163 (2019) 114866.
[56] W.D. Oh, Z. Dong, T.T. Lim, Generation of sulfate radical through heterogeneous catalysis for organic contaminants removal: current development, challenges and prospects, Appl. Catal. B-Environ. 194 (2016) 169–201.
[57] J. Deng, Y.S. Shao, N.Y. Gao, S.J. Xia, C.Q. Tan, S.Q. Zhou, X.H. Hu, Degradation of the antiepileptic drug carbamazepine upon different UV-based advanced oxidation processes in water, Chem. Eng. J. 222 (2013) 150–158.
[58] W.X. Qin, G.D. Fang, Y.J. Wang, T.L. Wu, C.Y. Zhu, D.M. Zhou, Efficient transformation of DDT by peroxymonosulfate activated with cobalt in aqueous systems: kinetics, products, and reactive species identification, Chemosphere 148 (2016) 68–76.